Regular Article

PHYSICAL CHEMISTRY RESEARCH
Published by the
Iranian Chemical Society
www.physchemres.org
info@physchemres.org

***Phys. Chem. Res.**, Vol. 4, No. 3, 315-332, September 2016*
DOI: 10.22036/pcr.2016.14142

Sensing Performance of Sc-doped $B_{12}N_{12}$ Nanocage for Detecting Toxic Cyanogen Gas: A Computational Study

M. Solimannejad[a,*], S. Kamalinahad[a] and E. Shakerzadeh[b]

[a]*Department of Chemistry, Faculty of Science, Arak University, 38156-8-8349, Arak, Iran*

[b]*Chemistry Department, Faculty of Science, Shahid Chamran University, Ahvaz, Iran*

(Received 6 February 2016, Accepted 1 April 2016)

Adsorption of cyanogen molecule on the surface of pristine and Sc-doped $B_{12}N_{12}$ nanocage is scrutinized using at DFT calculations to investigating its potential as chemical nanosensors. The results show that cyanogen is weakly adsorbed on the pristine $B_{12}N_{12}$ and consequently its electrical properties are changed insignificantly. In order to improve the properties of the nanocage sensor, Sc doping process was investigated. The obtained results show that doping process changes electrical properties of $B_{12}N_{12}$ dramatically. Furthermore, adsorption of the cyanogen on the exterior surface of Sc-doped $B_{12}N_{12}$ proves strong physisorption with E_{ads} equal to -73.20 kJ mol^{-1}. UV-Vis spectra display new absorption peaks confirming sensing ability of Sc-doped $B_{12}N_{12}$ for detection of the cyanogen molecule. Desired nanosensor has short recovery time because adsorption energy of NCCN molecule is not too large. It is expected that Sc-doped $B_{12}N_{12}$ acts as new potential nanosensor to detect toxic cyanogen molecule.

Keywords: Sensing of cyanogens, $B_{12}N_{12}$, Sc-doped $B_{12}N_{12}$, Density of state, DFT

INTRODUCTION

Cyanogen (NCCN) is colorless, toxic and flammable gas with an odor of almonds. It was first prepared by Gay-Lussac in 1815 by the thermal decomposition of silver cyanide [1]. Cyanogen is an important interesting material in the chemical industry as a high energy fuel (heat of formation = 73.8 kcal mol^{-1}) [2] for several applications. However, cyanogen is highly poisonous, having toxicity comparable to hydrogen cyanide. Cyanogen gas is an irritant to the eyes and respiratory system. Inhalation can make a headache, dizziness, rapid pulse, nausea, vomiting, and loss of consciousness, convulsions, and death, depending on exposure. The maximum permissible vapor concentration is 10 parts per million [3,4]. Thus, the design of the cyanogen nanosensors is highly important for monitoring cyanogen concentration in the environment.

*Corresponding author. E-mail: m-solimannejad@araku.ac.ir

Boron nitride (BN) compounds are able to form nanosize structures such as fullerene like cages, onions, and tubes. BN nanomaterials are anticipated in future application because they provide good stability at high temperatures with high electronic insulation in air [5], low dielectric constant, large thermal conductivity, and oxidation resistance [6]. Therefore, B_nN_n structures have been widely studied both theoretically and experimentally and $B_{12}N_{12}$ appears to be more stable one in comparison to others [7]. Oku *et al.* [8] synthesized $B_{12}N_{12}$ nanocage, detected by laser desorption time of the flight mass spectrometry. They showed that $B_{12}N_{12}$ clusters consisted of 4- and 6-membered rings of BN.

Nanotechnology is defined as the ability to manage and control individual atoms and molecules in the nanoscale which are leading to the design and fabrication of real-life functional, physical, chemical and biological systems. Nanotechnology offers a host of the new materials and novel functionalities that can be used for biological and chemical sensors. In many cases, materials in the nanoscale

have unusual optical, magnetic, catalytic and mechanical properties, greatly different from their bulk material counterparts [9,10]. These unique properties are lead to be utilized for the development of novel sensors and transduction systems by improving spatial resolution, reduced detection volumes, higher sensitivity levels, and faster response times [11,12].

Several studies on the adsorption of different molecules such as aniline [13], pyridine [14], urea [15], carbon dioxide [16], nitrogen dioxide [17], ammonia [18], carbon monoxide [19], methylamine [20], amphetamine [21], methanol [22], hydrogen cyanide [23], alkaline earth cations [24], fluorine atoms [25] and transition metal atom [26] on the $B_{12}N_{12}$ nanocage, have been reported. Recently, Li *et al*. [27] have exhibited that substitution the B atom of BNNTs with Sc atom is the most energetically favorable among all of the 3d transition metals. The adsorption of the cyanogen molecules on the surface of boron nitride nanosheet (BNNS) has been investigated on the previous study [28]. The results show that the absorption of cyanogen on Al and Si-doped BNNS is very strong and its recovery time is large. The main contribution of the present study is to examine the potential possibility of pristine and Sc-doped $B_{12}N_{12}$ nanocage as a new promising sensor for detection of the toxic cyanogen molecule.

COMPUTATIONAL METHODS

The adsorptions of cyanogen over the pristine and Sc-doped $B_{12}N_{12}$ nanocages have been studied within the framework of density functional theory (DFT). It is noteworthy that B3LYP is the conventional approach for investigating the nanostructures [29-32]. Nevertheless, it is unsuccessful at the calculation of the noncovalent interactions, and that is the incentive of using other mentioned functionals in this work. The Coulomb-attenuating method CAM-B3LYP is functional taking long-range correction to account has been proved to be appropriate for electronic properties [33,34]. Hence, the geometries were fully optimized using the new density functional, Coulomb-attenuated hybrid exchange-correlation functional (CAM-B3LYP) [34] of the density functional theory (DFT) [35] with the standard 6-31+G(d) basis set. The harmonic vibrational frequencies were also calculated to prove an optimized geometry properly fits to a local minimum that has only real frequencies. The charge transfer between the nanocage and the adsorbed molecules was calculated by using natural bond orbitals (NBO) analysis [36]. All calculations were carried out using the Gaussian09 package [37].

The quantum molecular descriptors [38] including energy gap (E_g), Fermi level energy (E_F), chemical potential (μ), hardness (η) and electrophilicity index (ω), were applied to study the considered system. The energy gap has the following operational equation:

$$E_g = (\text{HOMO} - \text{LUMO}) \quad (1)$$

where HOMO and LUMO are the highest occupied molecular orbital and the lowest unoccupied molecular orbital energies, respectively. The conventional assumption for a Fermi level (E_F) is in the middle of the energy gap (Eg) of molecule at 0 K approximately. Indeed, Parr *et al*. [39] explained that μ and η could be considered as the first and second partial derivatives of the electronic energy (E) with respect to the number of electrons (N) at a fixed external potential ($\nu(r)$), respectively. According to the Janak's approximation [40], their analytical and operational definitions are as follows:

$$\mu = \left(\frac{\partial E}{\partial N}\right)_{\nu(\vec{r}),T} \cong \frac{(\varepsilon_L + \varepsilon_H)}{2} \quad (2)$$

$$\eta = \frac{1}{2}\left(\frac{\partial^2 E}{\partial N^2}\right)_{\nu(\vec{r}),T} \cong \frac{(\varepsilon_L - \varepsilon_H)}{2} \quad (3)$$

Parr *et al*. [41] has introduced an index for the electrophilicity power of a system in connection with the chemical potential and hardness as:

$$\omega = \frac{\mu^2}{2\eta} \quad (4)$$

In fact, electrophilicity index is meant to be a measure of the energy lowering of the chemical species because of

maximum electron flow from the environment and could be considered as a measure of the capacity of species to receive desired electronic charge. Total density of states (TDOS) and partial density of states (PDOS) analyses were carried out on the pristine and Sc-doped $B_{12}N_{12}$ and different NCCN-$B_{12}N_{12}$ complexes at the same level of theory using the GaussSum program [42].

The adsorption energy (E_{ads}) of cyanogen on the surface of pristine and Sc-doped $B_{12}N_{12}$ was defined as:

$$E_{ads} = E_{complex} - E_{NCCN} - E_{BN\ nanocage} + E_{BSSE} \quad (5)$$

where $E_{complex}$, E_{NCCN} and $E_{BN\ nanocage}$ are total energies of pristine and Sc-doped $B_{12}N_{12}$ with adsorbed molecules, isolated NCCN and the pristine and Sc-doped $B_{12}N_{12}$, respectively. The basis set superposition error (BSSE) [43] was also evaluated using counterpoise method to eliminate basis functions overlap effects. Based on the Eq. (5), negative adsorption energy indicates that the formed complex is stable.

In order to investigate the thermodynamic feasibility of the cyanogen adsorption on the pristine and Sc-doped $B_{12}N_{12}$, we have computed the changes of the free energies (ΔG_{ads}) and enthalpies (ΔH_{ads}) at 298.14 K and 1 atmosphere defined as follows:

$$\Delta H_{ads} = H_{complex} - H_{NCCN} - H_{BN\ nanocage} \quad (6)$$

$$\Delta G_{ads} = \Delta H_{ads} - T\Delta S_{ads} = \Delta H_{ads} - T\ (S_{complex} - S_{NCCN} - S_{BN\ nanocage} \quad (7)$$

where H and S are thermal enthalpy and entropy, respectively.

To assess the stability of pristine and Sc-doped $B_{12}N_{12}$ nanocages, we calculated the binding energy (E_b) using the following expression, as this trend has previously been used by Wang *et al*. [44].

$$E_b = [E_{tot} - n(E_X)]/N \quad (8)$$

where E_{tot} is the total energy of the pristine and Sc-doped $B_{12}N_{12}$ nanocage, n is the number of B, N and Sc atoms involved, E_X is the energies of an isolated B, N and Sc atom, respectively, and N is total of atoms involved. The UV-Vis spectra of complex forms of NCCN/$B_{12}N_{12}$ cage was simulated at TD-CAM-B3LYP/6-31+G(d) level of theory [45].

RESULTS AND DISCUSSION

Structural Optimization and Geometry of Pristine $B_{12}N_{12}$

The structural optimization of pristine $B_{12}N_{12}$ is performed at CAM-B3LYP level with 6-31+G(d) basis set. $B_{12}N_{12}$ includes six tetragonal and eight hexagonal BN rings with T_h symmetry. $B_{12}N_{12}$ has two nonequivalent B-N bonds: one is shared between a tetragonal and a hexagonal ring and the other between two hexagonal rings. The calculated bond lengths of these bonds are 1.481 and 1.434 Å, respectively (see Fig. 1a). These results are in good agreement with the previous studies [46]. Also, NBO analysis shows that natural charge of N atom in $B_{12}N_{12}$ is about -1.174 |e|, because of the difference between electronegativity of N atom with respect to B atom. These results confirm the partial ionic character of B-N bond. The electronic properties of this nanocage are also studied. The obtained frontier molecular orbital energies (HOMO and LUMO) and the computed energy gap (E_g) values for the considered nanocage are shown in Table 1. The outcome energy gap for the $B_{12}N_{12}$ is about 9.58 eV (Table 1). The total density of state (TDOS) and graphical presentation of the HOMO and LUMO distribution of pristine $B_{12}N_{12}$ is present in Figs. 1c and 4. According to Fig. 4, the HOMO is concentrated on the N atoms of the nanostructures and the LUMO is spread over the B atoms. The calculated value of binding energy (E_b) for pristine $B_{12}N_{12}$ is about -577.61 kJ mol^{-1}, suggesting that the $B_{12}N_{12}$ may be a stable substance. Also, the optimized structure of the cyanogen molecule is depicted in Fig. 1b. According to this figure, the NCCN molecule is linear; the calculated bond length of N≡C and C-C is about 1.386 and 1.156 Å, respectively. These results are quite consistent with the experimental results [47].

Cyanogen Adsorption on the Pristine $B_{12}N_{12}$

In order to find the most stable configurations of the adsorbed cyanogen on the exterior surface of the $B_{12}N_{12}$ nanocage, different possible adsorption structures were examined. The molecular electrostatic potential (MEP)

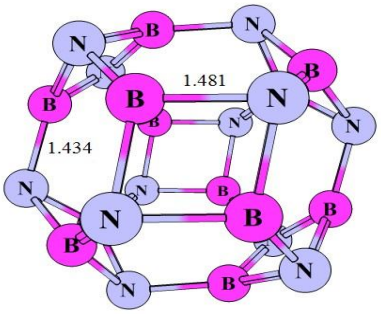

(a)

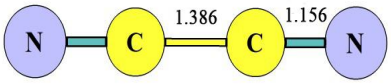

(b)

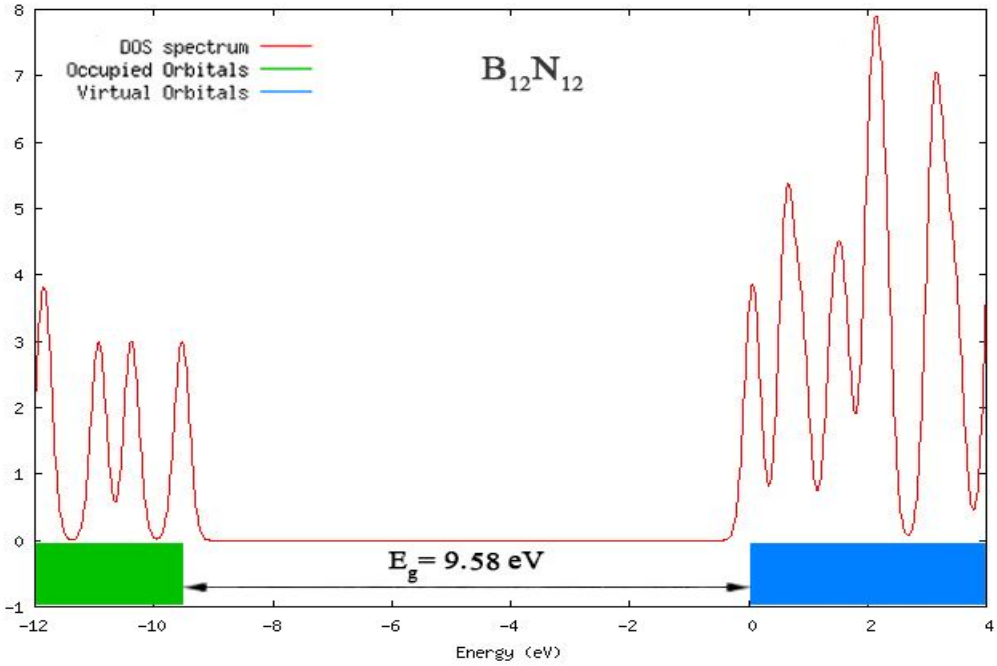

(c)

Fig. 1. Optimized structure of $B_{12}N_{12}$, NCCN and total density of states (TDOS) of $B_{12}N_{12}$ (Bonds in Å).

surfaces of the cyanogen are shown in Fig. 2. It can be seen that the electron density (red color in Fig. 2) is localized on the N atoms of cyanogen. Thus, cyanogen can be approach to the nanocage by the N atom. Finally, two stable adsorption configurations are observed, containing (see Fig. 3): (A) the nitrogen atom in the NCCN molecule is bonded with B atom of the external surface of the $B_{12}N_{12}$, (B) C-C bond in the cyanogen is placed in parallel on N atom of $B_{12}N_{12}$. The calculated E_{ads} and BSSE values for two configurations using Eq. (5) are listed in Table 2. According to the results of this table, E_{ads} values for A and B configurations are -7.06 and -4.98 kJ mol^{-1}, respectively. Negative values of adsorption energy indicate the structures are stable though the interaction between cyanogen

Table 1. Highest Occupied Molecular Orbital (HOMO), Lowest Unoccupied Molecular Orbital (LUMO), Energy Gap (E_g), the Change of Energy gap of Nanocage after Adsorption (ΔE_g (%)) and Fermi Level Energies (E_F) for NCCN Adsorbed on the Pristine and Sc-doped $B_{12}N_{12}$

Configuration	HOMO (eV)	LUMO (eV)	E_g (eV)	ΔE_g (%)	E_F (eV)
$B_{12}N_{12}$	-9.53	0.05	9.58	-	-4.74
A	-9.34	-1.67	7.67	-19.91	-5.51
B	-9.59	-1.31	8.28	-13.55	-5.45
$ScB_{11}N_{12}$	-8.61	-1.82	6.79	-	-5.22
C	-8.30	-3.50	4.79	-29.35	-5.90
$B_{12}N_{11}Sc$	-6.89	-1.79	5.10	-	-4.34
D	-6.52	-3.39	3.13	-38.35	-4.96

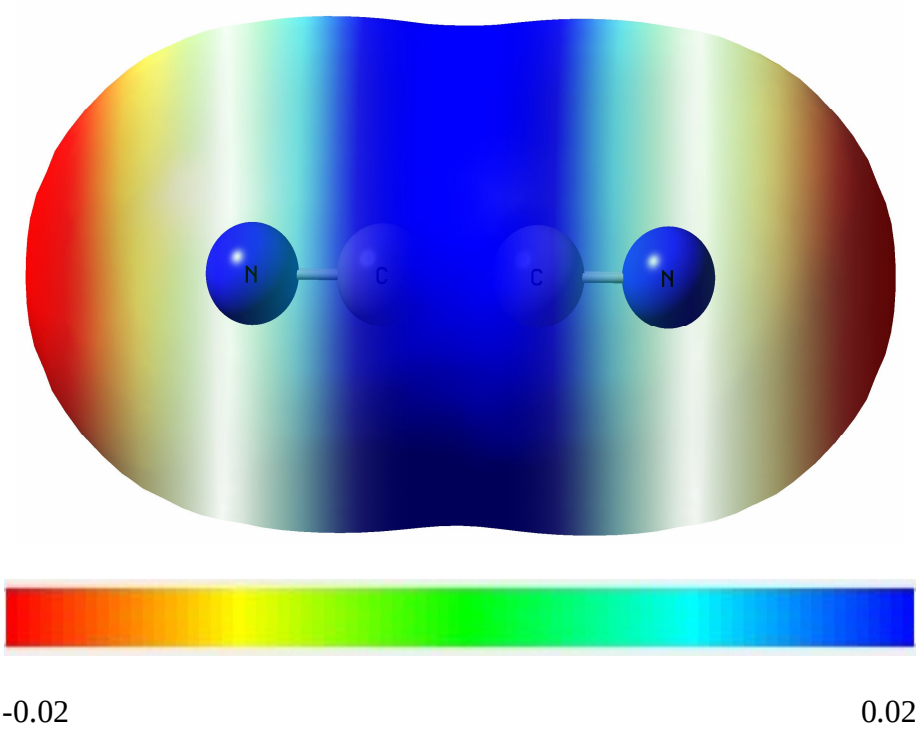

Fig. 2. Molecular electrostatic potential surface of the cyanogen molecule. The surfaces are defined by the 0.0004 electrons/b^3 contour of the electronic density. Color ranges in a.u.

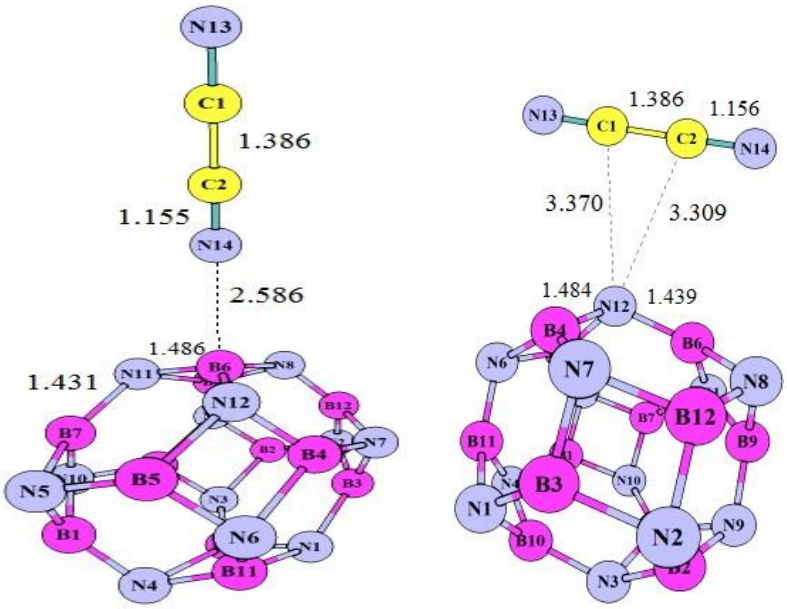

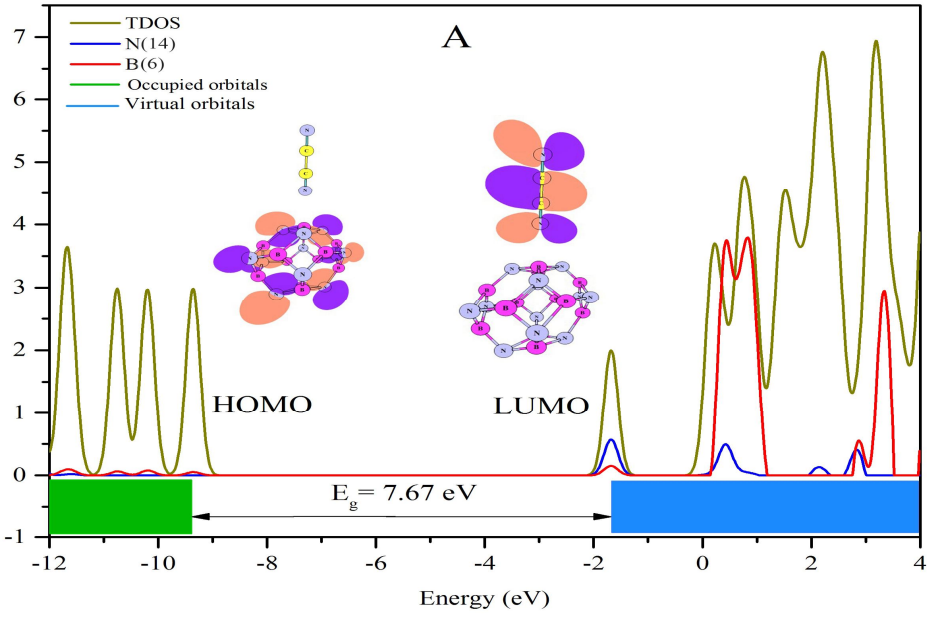

Fig. 3. Optimized structure of A and B configurations and total density of states (TDOS) and partial density of states (PDOS) of A configuration (Bonds in Å).

Table 2. Charge Transfer from Molecule to Cage (Q_T) and Adsorption Energy (E_{ads}), BSSE, Calculated Thermodynamic Properties at 298 K and 1 atm (ΔH_{ads}, ΔS_{ads} and ΔG_{ads}), Electronic Chemical Potential (μ), Hardness (η) and Electrophilicity (ω) of the Pristine and Sc-doped $B_{12}N_{12}$, A, B, C and D Configurations

Configuration	Q_T (me)	E_{ads} (kJ mol^{-1})	BSSE (kJ mol^{-1})	ΔH_{ads} (kJ mol^{-1})	ΔS_{ads} (J mol^{-1} k^{-1})	ΔG_{ads} (kJ mol^{-1})	μ	η	ω
$B_{12}N_{12}$	-	-	-	-	-	-	-4.74	4.79	2.35
A	53	-7.06	2.82	-5.53	-75.60	17.00	-5.51	3.83	3.95
B	3	-4.98	1.51	-2.07	-57.64	15.12	-5.45	4.14	3.59
$ScB_{11}N_{12}$	-	-	-	-	-	-	-5.22	3.39	4.01
C	133	-73.20	3.95	-72.89	-107.72	-40.77	-5.90	2.40	7.26
$B_{12}N_{11}Sc$	-	-	-	-	-	-	-4.34	2.55	3.69
D	46	-56.27	2.99	-56.07	-95.64	-27.56	-4.96	1.57	7.83

molecule and $B_{12}N_{12}$ is very weak. In the A configuration, the B-N distance is 2.586 Å, while in the B configuration, the N-C distances are 3.309 and 3.370 Å, respectively (see Fig. 3). As shown in Table 2, a partially charge transfer from cyanogen to $B_{12}N_{12}$ is occurred when cyanogen molecule adsorbed on $B_{12}N_{12}$. Based on the results of this table, a small charge transfer (53 |me|) occurs in A configuration. In addition, in B configuration, charge is transferred slightly (3 |me|) from cyanogen to $B_{12}N_{12}$. These results indicate that the weak electrostatic interaction between cyanogen and $B_{12}N_{12}$ is occurred and the adsorption of cyanogen on the $B_{12}N_{12}$ is a physisorption process.

In order to inspect the effect of adsorption of NCCN on the electronic properties of the $B_{12}N_{12}$ nanocage, the electronic properties of the nanocage/cyanogen system such as HOMO-LUMO gap energy and Fermi level energy (E_F) show a small change (see Table 1). Table 1 implying the Eg in the A and B configurations are 7.67 and 8.22 eV, respectively. The small shift of Eg (ΔEg) within the adsorption process is related to the weak adsorption on the external surface of pristine $B_{12}N_{12}$. Typically, graphical presentation of the HOMO and LUMO distribution of A configuration are shown in Fig. 4. According to this figure, the HOMO is concentrated on the nanocage and the LUMO is spread over the cyanogen molecule. This phenomenon is in agreement with the charge transfer of cyanogen to nanocage. To examine the effects of the absorption of the cyanogen on the electronic properties of the $B_{12}N_{12}$, TDOS and PDOS calculations are analyzed for configuration A of NCCN/$B_{12}N_{12}$ (see Fig. 3). It is clarified from PDOS analysis that there is an interaction between B(6) with N(14) in A configuration (atom numbering is depicted in Fig. 3) and small new peak is appeared farther than the Fermi level (-1.67 eV) because of the interaction between the cyanogen molecule and the nanocage. In this case the band gap of the A decreases by 19.91% and the conductivity of the system is slightly changed. Therefore, this nanocage is not sensitive enough for sensing cyanogen molecule.

The thermodynamic possibility for an adsorption of the cyanogen on surface of the $B_{12}N_{12}$ is investigated. The changes of enthalpies (ΔH_{ads}), Gibbs free energies (ΔG_{ads}), and entropies (ΔS_{ads}) of the A and B configurations are calculated from the frequency calculations according to Eqs. (6) and (7) which is listed in Table 2. In this table, values of ΔH_{ads} for A and B configurations are -5.53 and -2.06 kJ mol^{-1}, while the values of ΔG_{ads} are 17.00 and 15.12 kJ mol^{-1}, respectively. These results

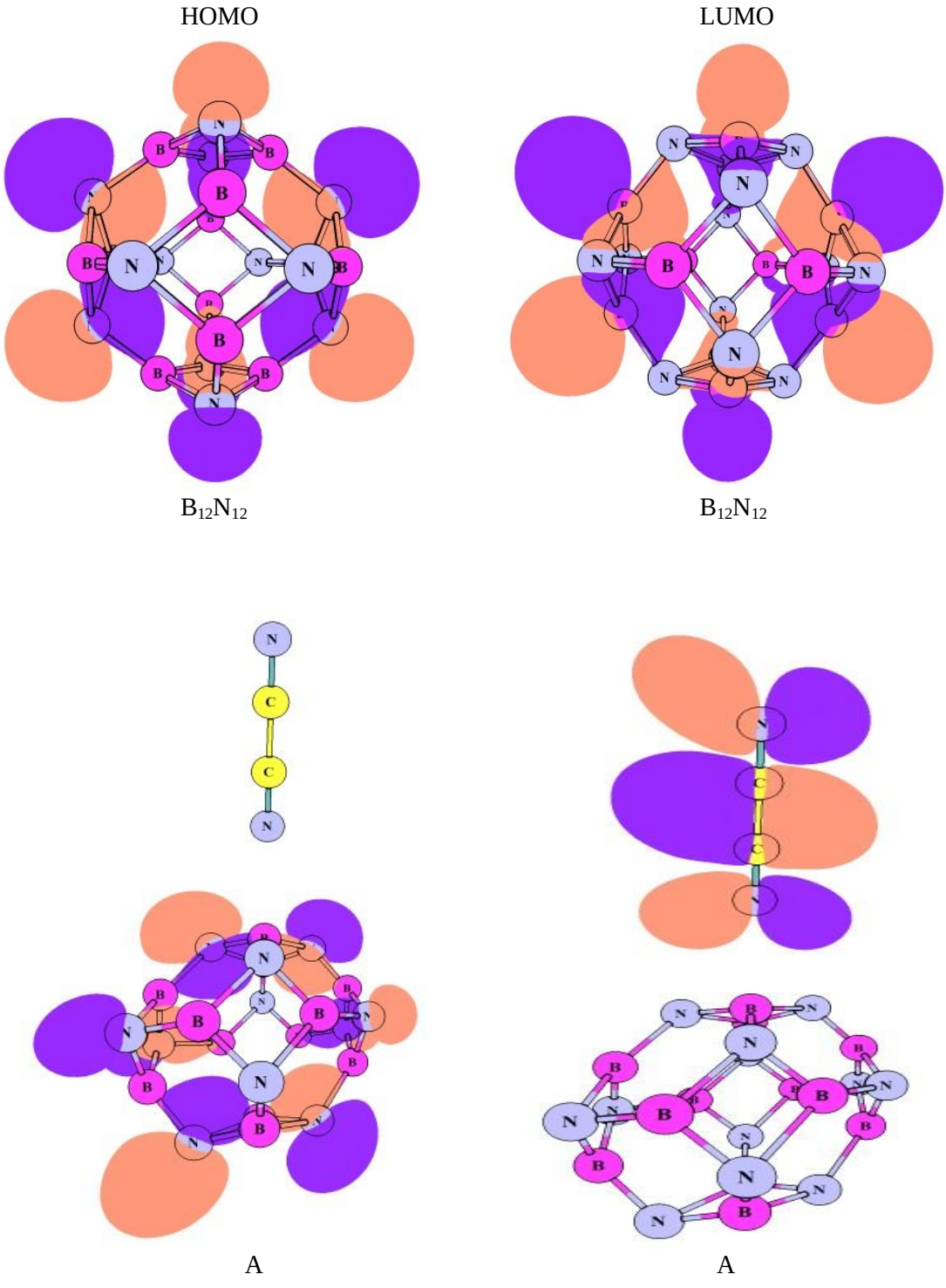

Fig. 4. HOMO and LUMO profiles of $B_{12}N_{12}$ and A configuration.

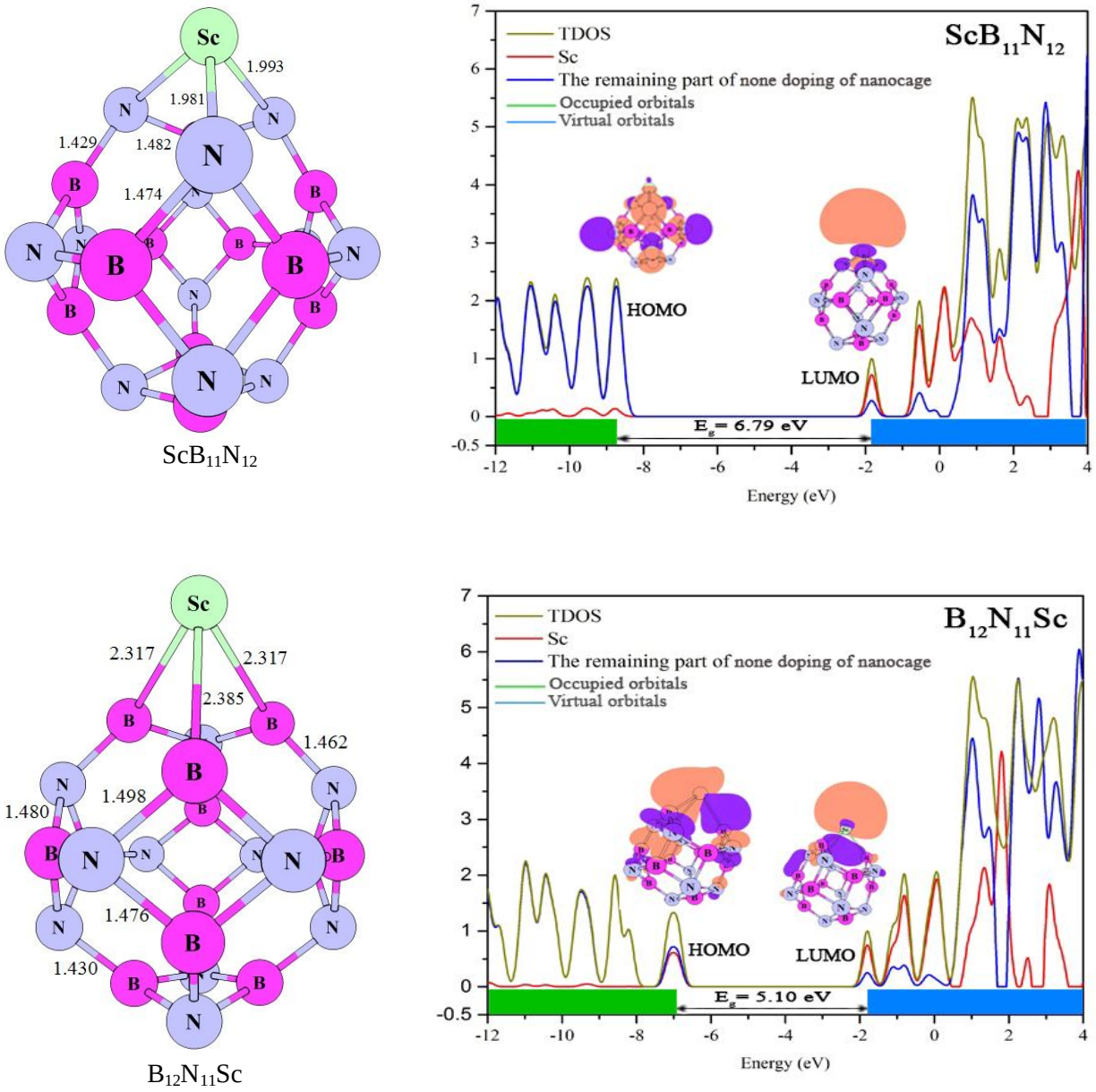

Fig. 5. Optimized structures, total density of states (TDOS) and partial density of states (PDOS) of $ScB_{11}N_{12}$ and $B_{12}N_{11}Sc$ (bond lengths are in Å).

conform the weakly physical adsorption of cyanogen on the exterior surface of $B_{12}N_{12}$. According to the global reactivity indices of the pristine $B_{12}N_{12}$ and NCCN (see Table 2), when the cyanogen molecule adsorbed on the surface of $B_{12}N_{12}$ the hardness values of the A and B configurations are decreased and the electronic chemical potential electrophilicity of these configurations are increased, indicating that the reactivity of the systems has been increased.

Structural Optimization of the Sc-doped $B_{12}N_{12}$

Although inherent conductivity of the nanostructures changes by physical adsorption, the weak interaction between gases and nanostructure show the unstable

Table 3. Selected Excitation Energies (ΔE), Wavelength (λ), Oscillator Strength (f_0), and Relative Orbital Contributions for Sc-doped $B_{12}N_{12}$, A, B, C and D Configurations

Configuration	Excited State	ΔE (eV)	Λ (nm)	f_0	Assignment
$ScB_{11}N_{12}$	8	5.22	237.45	0.0280	HOMO ⟶ LUMO
	(3)	(4.62)	(268.46)	(0.0142)	(HOMO ⟶ LUMO+2)
C	6	3.49	355.58	0.0515	HOMO -2 ⟶ LUMO+1
	(2)	(3.13)	(395.81)	(0.0356)	(HOMO-1 ⟶ LUMO)
$B_{12}N_{11}Sc$	4	2.39	519.74	0.0132	HOMO ⟶ LUMO+1
	(8)	(2.72)	(456.07)	(0.0130)	(HOMO-1 ⟶ LUMO+5)
D	9	2.65	467.67	0.0072	HOMO-2 ⟶ LUMO

configuration at room temperature and small change of electronic structure [48]. The doping process can make a great impact on changing the electrical properties and gas sensing of the nanostructures [49,50]. It is suggested that Sc-doped BNNTs may be used as a promising gas sensor for monitoring the phosgene [51]. In order to improve the efficiency of the cyanogen nanosensor, we have examined the effect of scandium doping in $B_{12}N_{12}$ nanocage. To this end, in $B_{12}N_{12}$ nanocage two separate locations (B or N) for doping with Sc atom are measured. In this nanocage a boron and nitrogen atom are substituted by Sc atom. The optimized structures of these doped $B_{12}N_{12}$ nanocage at the CAM-B3LYP/6-31+G(d) level of theory are displayed in Fig. 5. It should be noted that the process of doping causes the local deformation of the all nanoclusters and the doped atoms are driven out of the plane due to reduce of torsional strain. The results show that in two doped nanocages, N-Sc and B-Sc bonds are larger than B-N bond, confirming the spread of geometries in optimized structures. Also, the bonding energy (E_b) was calculated for Sc-doped $B_{12}N_{12}$. The calculated values for $ScB_{11}N_{12}$ and $B_{12}N_{11}Sc$ are about -570.53 and -548.73 kJ mol^{-1}, respectively, suggesting that Sc-doped $B_{12}N_{12}$ could be thermodynamically stable likewise pristine $B_{12}N_{12}$. The obtained frontier molecular orbital energies (HOMO and LUMO) and the computed energy gap (Eg) and Fermi level energies (E_F) values of the doped nanocages are listed in Table 1. The results of this table obviously show that doped atom narrows the wide energy gap (Eg) of $B_{12}N_{12}$ nanocage in the range of 2.69-4.38 eV; the total density of state (TDOS) and partial density of state (PDOS) of doped nanocages are represented in Fig. 5. According to this figure, doping of B and N with Sc in $B_{12}N_{12}$ leading to HOMO orbital with the upper energy and LUMO orbital with the lower energy, so the energy gap between HOMO and LUMO are reduced. The results of PDOS display that new HOMO level is appeared from none-doped part of the nanocage while Sc-doped atom forms new LUMO level (Fig. 5). Therefore, doping Sc atom can effectively reduce the energy gap of $B_{12}N_{12}$. The TD-DFT calculations are performed to get the crucial excited states of Sc-doped $B_{12}N_{12}$ with the largest oscillator strength. The results are summarized in Table 3 and Fig. 7. The TD-DFT results display that its crucial excited state is composed of many components, at which the main components are the HOMO ⟶ LUMO and HOMO ⟶ LUMO + 2 transitions for $ScB_{11}N_{12}$ as well as

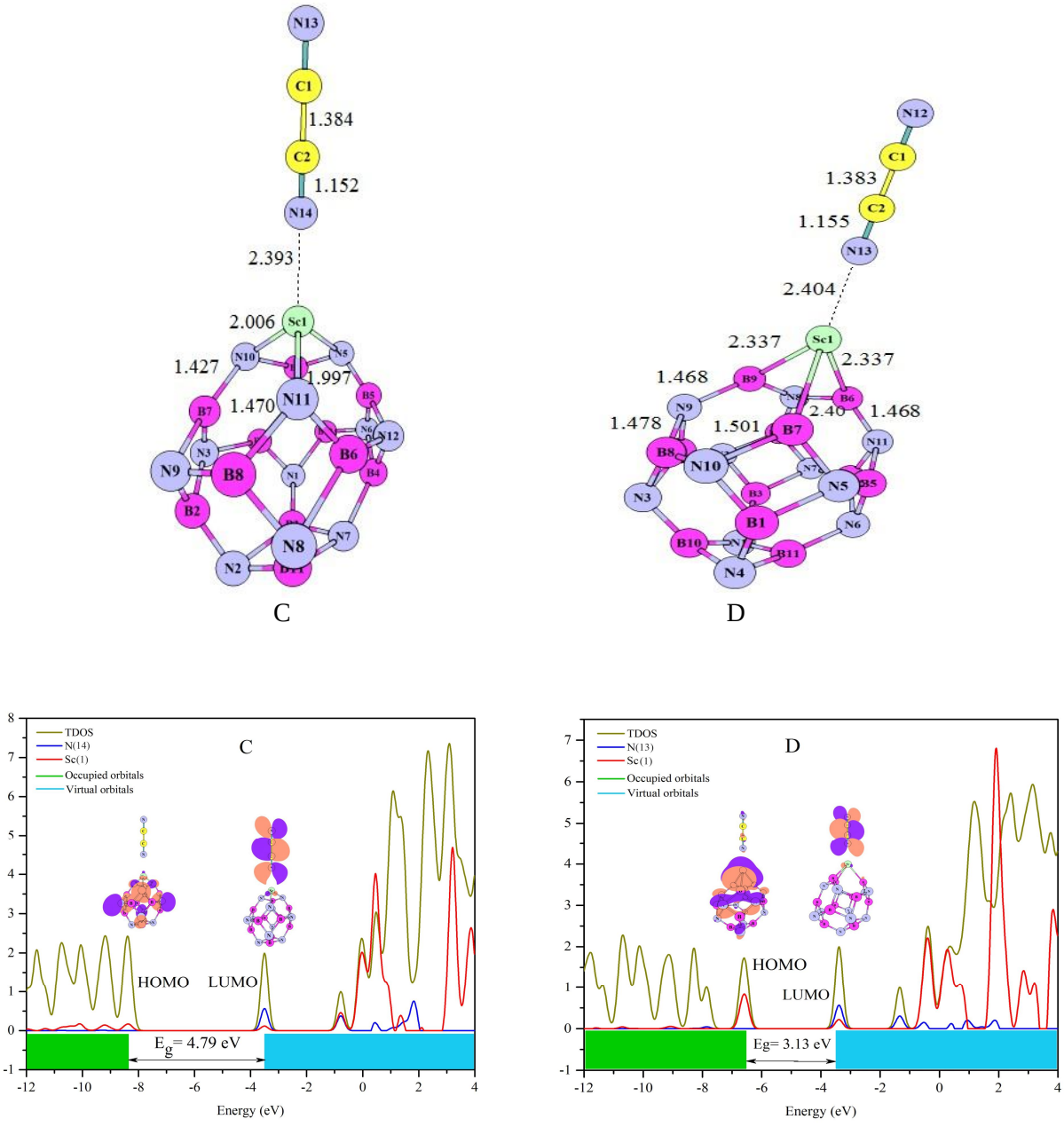

Fig. 6. Optimized structure, total density of states (TDOS) and partial density of states (PDOS) of C and D configurations (bond lengths are in Å).

the HOMO ⟶ LUMO+1 and HOMO-1 ⟶ LUMO+5 transition for $B_{12}N_{11}Sc$. Obviously, small transition energy is a determining factor and leads to a considerably reduced energy gap of Sc-doped $B_{12}N_{12}$. The calculated linear absorption spectra of $ScB_{11}N_{12}$ and $B_{12}N_{11}Sc$ are depicted in Fig. 8. There is significant different between UV-Vis spectrum of these two structures. For $ScB_{11}N_{12}$, the major absorption peak is at 268.46 nm in the UV, while in the $B_{12}N_{11}Sc$ spectrum, the strongest peak at 519.74 nm is in the visible region, corresponding to the transition of HOMO ⟶ LUMO and HOMO ⟶ LUMO+1, respectively (see Fig. 8). Moreover, for $ScB_{11}N_{12}$, there is

an additional peak at 237.45 nm in the UV region corresponding to the transitions of the HOMO ⟶ LUMO + 2. For $B_{12}N_{11}Sc$, another peak can be seen at 456.07 nm in the visible region, that is proportional to the HOMO-1⟶ LUMO + 5 transitions. Moreover the results of hardness and electrophilicity values for these doped $B_{12}N_{12}$ nanocage display the chemical stability and electrophilic character of these systems. Because of doping Sc atom, the reactivity and electrophilic power of these nanocage are enhanced compared with those of pristine $B_{12}N_{12}$ (see Table 2).

Cyanogen Adsorption on the Sc-doped $B_{12}N_{12}$

In the following, we investigate the NCCN adsorption on the Sc-doped $B_{12}N_{12}$ in several positions. After relax optimization of initial structures, only two stable structures were obtained: C and D configurations at which the nitrogen atom in the NCCN molecule is bonded to Sc atom of the external surface of the Sc-doped $B_{12}N_{12}$. For better vision, optimized structures are shown in Fig. 6. In the C and D configurations, the Sc-N distance are 2.393 and 2.404 Å, respectively (see Fig. 6). The computed E_{ads} and BSSE values for two configurations using Eq. (5) are summarized in Table 2. The results of this table, E_{ads} values for C and D configurations are -73.20 and -56.27 kJ mol^{-1}, respectively. Negative values of the adsorption energy indicate that the structures are stable; however the interaction between cyanogen molecule and Sc-doped $B_{12}N_{12}$ is a strong physisorption process. According to the obtained results above, the adsorption process in the configuration C is stronger than that of the D one. It is clear that Sc-doped $B_{12}N_{12}$ and cyanogen molecule are natural and after adsorption of cyanogen on the exterior surface of Sc-doped $B_{12}N_{12}$ charge transfer occurs. According to the results reported in Table 2, charge transfer of 133 and 46 |me| occurs from cyanogen to the Sc-doped $B_{12}N_{12}$, confirming the stronger interaction.

To investigate the effect of NCCN adsorption on the electronic properties of the Sc-doped $B_{12}N_{12}$ nanocage, the electronic properties of C and D configurations such as HOMO, LUMO, energy gap and Fermi level energy (E_F) show a significant change (see Table 1). As shown in Table 1, Eg of the C and D configurations are 4.79 and 3.13 eV, respectively. During the adsorption process, the significant shift of Eg (ΔEg) has been occurred proportional to the strong adsorption on the external surface of Sc-doped $B_{12}N_{12}$. In order to inspect the effects of the absorption of cyanogen on the electronic properties of the Sc-doped $B_{12}N_{12}$, TDOS and PDOS calculation are analyzed for C and D configurations (see Fig. 6). It is obvious that interaction between Sc(1) with N(14) and N(13) in C and D configurations, respectively, is confirmed from PDOS (atom numbering is depicted in Fig. 6). New band is appeared near to the Fermi level of $ScB_{11}N_{12}$ and $B_{12}N_{11}Sc$ (-3.59 and -3.39 eV, respectively) because of the interaction between cyanogen molecule and the Sc-doped nanocage. Also we can see from TDOS plots that their valence and conduction levels in both of the C and D configurations significantly shift upwards and downwards, respectively. In addition, the results of PDOS show that Sc-doped atom is more involved in the production of new LUMO level (Fig. 6), so that the E_g value of the Sc-doped $B_{12}N_{12}$ is significantly decreased by 28.35 and 38.35%, respectively, and the conductivity of the system significantly is changed. Therefore, Sc-doped nanocage especially $ScB_{11}N_{12}$, can be good candidate for physisorption sensing cyanogen molecule.

The crucial transition state with the largest oscillator strength and transition energies (ΔE) of the C and D configurations obtained at the TD-CAM-B3LYP/6-31+G(d) level of theory are illustrated in Table 3 and Fig. 7. According to this figure, the electron cloud in LUMO and LUMO+1 are dominant over the cyanogen molecule, while electron clouds in HOMO-1 and HOMO-2 orbitals are spread over the Sc-doped $B_{12}N_{12}$ nanocage. The small transition energies (ΔE) of the crucial excited states for C and D configurations lead to a considerably reduced energy gap of these configurations. Furthermore, UV-Vis spectra for the C and D configurations are given in Fig. 8. Look at these spectra, there is a considerable difference in those two spectra with Sc-doped nanocage. Compared with the absorption strength of $ScB_{12}N_{12}$, the absorption strength of C configuration significantly increases with red shift effects, which corresponds to the transition of HOMO-2⟶LUMO+1 at 355.58 nm in the UV region and HOMO-1 ⟶ LUMO at 395.81 nm in the visible region. It is obvious that in spectrum of D configuration two absorption peaks at 519.74 and 456.07 nm are removed and one new peak is generated at 467.67 nm in visible region

after adsorption of cyanogen molecule. This new observation peak corresponds to HOMO-2 ⟶ LUMO transition. This observation implies to interaction between cyanogen and nanocage and charge transfer from cage to cyanogen molecule.

Also in this study, the thermodynamic possibility of adsorption cyanogen on the surface of Sc-doped $B_{12}N_{12}$ is inspected. The changes of enthalpies (ΔH_{ads}), Gibbs free energies (ΔG_{ads}), and entropies (ΔS_{ads}) of the C and D configurations are computed from the frequency calculations according to Eqs. (6) and (7), and the results are summarized in Table 2. According to this table, values of ΔH_{ads} for C and D configurations are -72.89 and -56.07 kJ $mol^{-1}$and corresponding ΔG_{ads}s are -40.77 and -27.56 kJ mol^{-1}, respectively. These results are indicative of physical adsorption of cyanogen on the exterior surface of Sc-doped $B_{12}N_{12}$ while adsorption on the $ScB_{11}N_{12}$ (C configuration) is stronger than that for the others. According to the global reactivity indices of the Sc-doped $B_{12}N_{12}$ and NCCN (see Table 2), when the cyanogen molecule adsorbed on the surface of Sc-doped $B_{12}N_{12}$ the hardness values of the C and D configurations are decreased and the electronic

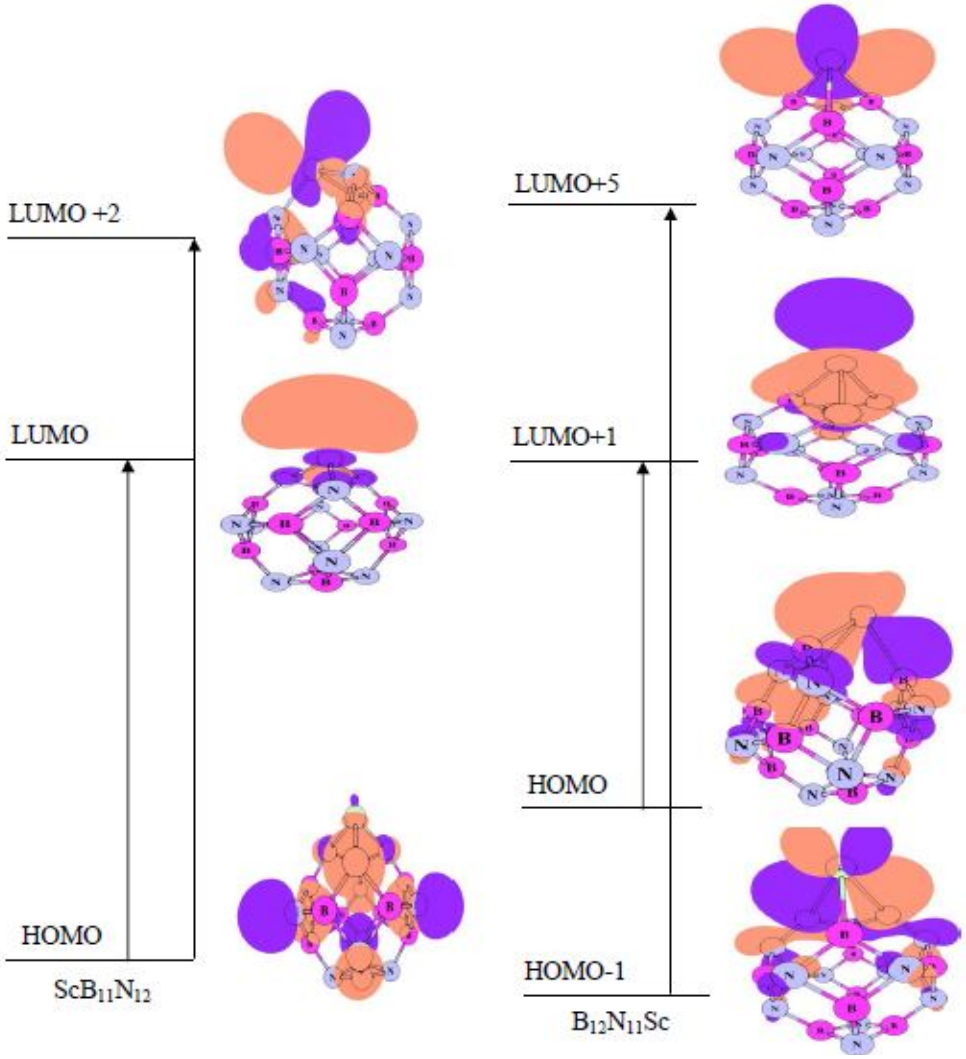

Fig. 7. Crucial transition states of $ScB_{11}N_{12}$, $B_{12}N_{11}Sc$, C and D configurations with the largest component coefficient marked.

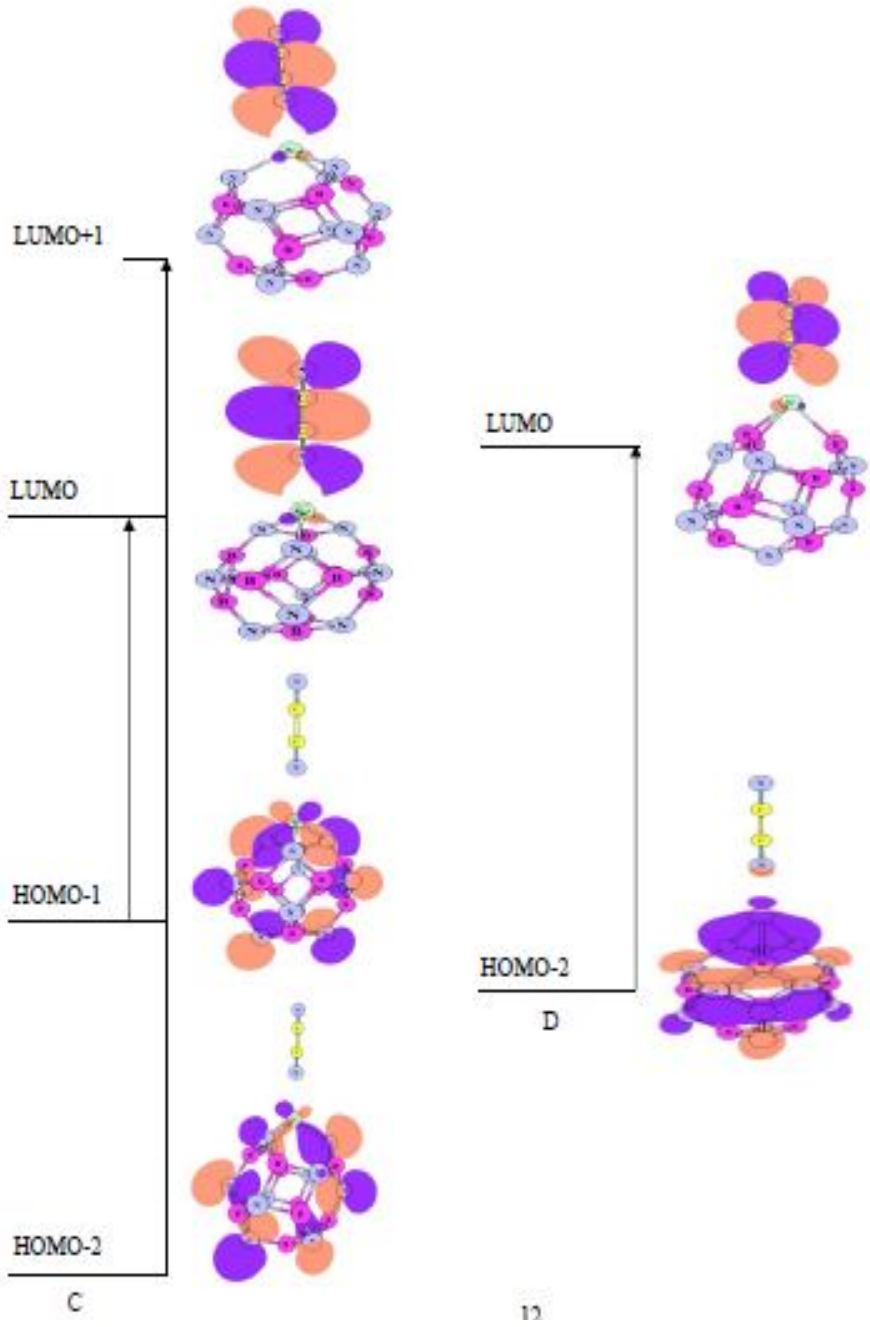

Fig. 7. Continued.

chemical potential and electrophilicity of these configurations are significantly increased, indicating that the reactivity of the systems are increased.

It is noteworthy that an important characteristic of the gas sensor is its recovery time. Such a strong interaction might be due to the difficulty and prolonged recovery time sensor for desorption of the adsorbate. With a significant increase in absorption energy, it is expected that the recovery time of sensor is prolonged. According to the conventional transition state theory, the recovery time can

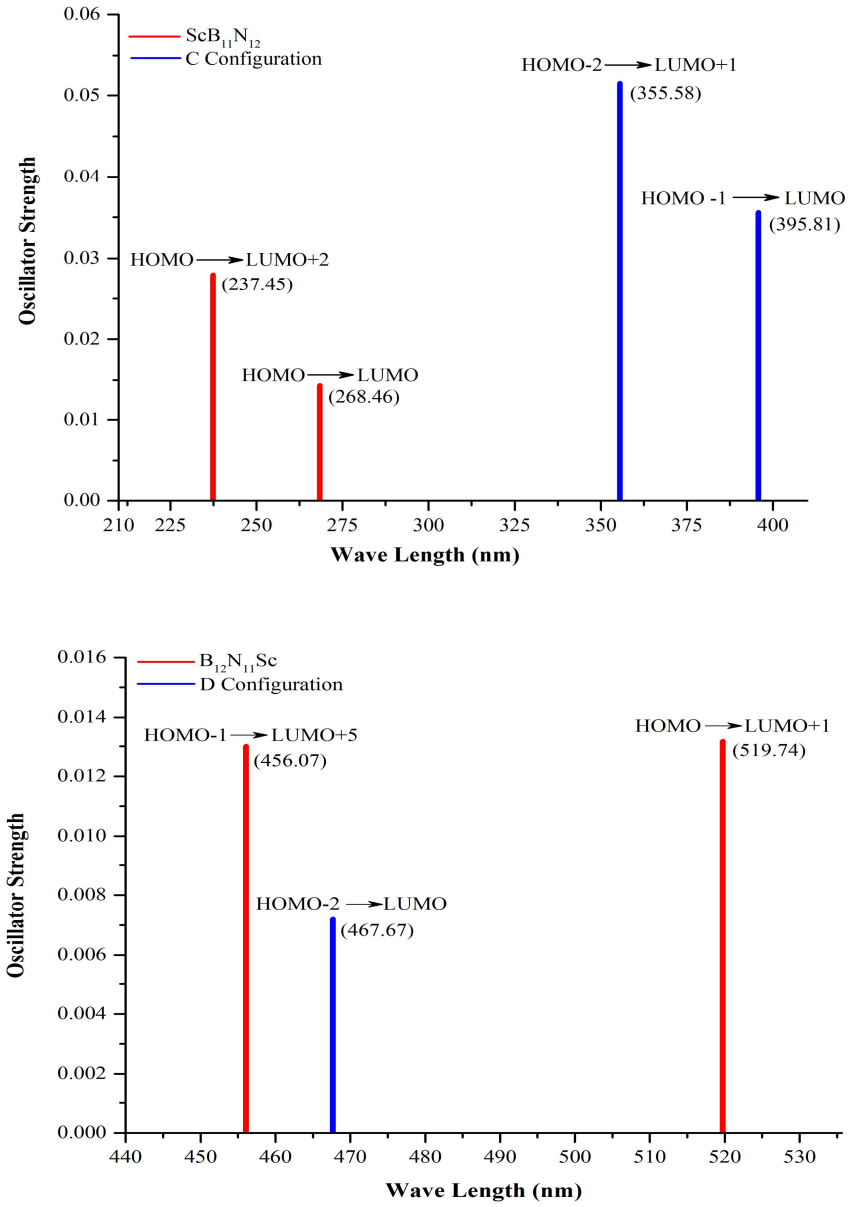

Fig. 8. UV-Vis spectra of the pristine ScB11N12, $B_{12}N_{11}Sc$, C and D configurations.

be expressed by the following equation [52]:

$$\tau = \nu_0^{-1} \exp(-E_{ads} / kT) \quad (9)$$

where T is the temperature, k is the Boltzmann's constant, and ν_0 is the attempt frequency. According to this equation, more negative E_{ads} values will lengthen the recovery time in an exponential manner. According to the results of this study, as a utility, the adsorption energy of the cyanogen is not too large to prevent the recovery of Sc-doped $B_{12}N_{12}$ and the recovery time may be is short according to the mentioned equation.

CONCLUSIONS

Using density functional theory, the adsorption of

cyanogen molecule on the pristine and Sc-doped $B_{12}N_{12}$ is investigated. The geometrical structures, electronic properties and NBO analysis are performed in the presence and absence of a cyanogen molecule to predict the adsorption properties of these complexes. The obtained results exhibit that cyanogen molecule interacts with the pristine $B_{12}N_{12}$ through weak van der Waals interactions implying the weak physisorption process. Interaction between Sc-doped $B_{12}N_{12}$ and the cyanogen molecule is strong physical adsorption with considerable changes in its electrical conductance. Accordingly, Sc-doped $B_{12}N_{12}$ is introduced as a promising nanosensor for detecting of cyanogen, due to some features such as short recovery time, high sensitivity and also energetic favorability. UV-Vis spectra display that cyanogen adsorption on the exterior surface of Sc-doped $B_{12}N_{12}$ leads to the change in the absorption peaks associated with the sensing of the cyanogen molecule.

REFERENCES

[1] Gay-Lussac, J. L., *Recherches sur l'acide prussique*. Imprimerie de Mme. Ve. Perronneau, **1815**.

[2] Brotherton, T.; Lynn, J., The synthesis and chemistry of cyanogen. *Chem. Rev.*, **1959**, *59*, 841-883. DOI: 10.1021/cr50029a003.

[3] Elkins, H. B., *The chemistry of industrial toxicology.*, **1959**, (2nd Edition).

[4] Renfew, M. M., NIOSH Pocket guide to chemical hazards (US Department of Health and Human Services-National Institute for Occupational Safety and Health). *J. Chem. Educ.*, **1991**, *68*, A232. DOI: 10.1021/ed068pA232.3.

[5] Oku, T.; Narita, I.; Koi, N.; Nishiwaki, A.; Suganuma, K.; Inoue, M.; Hiraga, K.; Matsuda, T.; Hirabayashi, M., Tokoro, H., *Boron nitride nanocage clusters, nanotubes, nanohorns, nanoparticles, and nanocapsules*. In: BCN Nanotubes and Related Nanostructures. Springer, **2009**, p. 149-194.

[6] Oku, T.; Kuno, M.; Kitahara, H., Narita, I., Formation, atomic structures and properties of boron nitride and carbon nanocage fullerene materials. *Int. J. Inorg. Mater.*, **2001**, *3*, 597-612. DOI: 10.1016/ S1466-6049(01)00169-6.

[7] Seifert, G.; Fowler, P.; Mitchell, D.; Porezag, D.; Frauenheim, T., Boron-nitrogen analogues of the fullerenes: electronic and structural properties. *Chem. Phys. lett.*, **1997**, *268*, 352-358. DOI: 10.1016/S0009-2614(97)00214-5.

[8] Oku, T.; Nishiwaki, A.; Narita, I., Formation and atomic structure of $B_{12}N_{12}$ nanocage clusters studied by mass spectrometry and cluster calculation. *Sci. Technol. Adv. Mat.*, **2004**, *5*, 635-638. DOI: 10.1016/ j.stam.2004.03.017.

[9] Yonzon, C. R.; Stuart, D. A.; Zhang, X.; McFarland, A. D.; Haynes, C. L.; Van Duyne, R. P., Towards advanced chemical and biological nanosensors-an overview. *Talanta*, **2005**, *67*, 438-448. DOI: 10.1016/j.talanta.2005.06.039.

[10] Bakker, E.; Qin, Y., Electrochemical sensors. *Anal. Chem.*, **2006**, *78*, 3965-3984. DOI: 10.1021/ ac060637m.

[11] Salam, M. A.; Al-Zhrani, G.; Kosa, S. A., Simultaneous removal of copper(II), lead(II), zinc(II) and cadmium(II) from aqueous solutions by multi-walled carbon nanotubes. *C. R. Chim.*, **2012**, *15*, 398-408. DOI: 10.1016/j.crci.2012.01.013.

[12] Kauffman, D. R.; Star, A., Carbon nanotube gas and vapor sensors. *Angew. Chem. Int. Ed.*, **2008**, *47*, 6550-6570. DOI: 10.1002/anie.200704488.

[13] Baei, M. T.; Mohammadian, H.; Hashemian, S., $B_{12}N_{12}$ nanocage as a potential adsorbent for the removal of aniline from environmental systems. *Bulg. Chem. Commun.*, **2014**, *46*, 735-742.

[14] Baei, M. T., Remove of toxic pyridine from environmental systems by using $B_{12}N_{12}$ nano-cage. *Superlattices. Microstruct.*, **2013**, *58*31-37. DOI: 10.1016/j.spmi.2013.02.009.

[15] Baei, M. T., Adsorption of the urea molecule on the B12N12 nanocage. *Turk. J. Chem.*, **2014**, *38*, 531-537. DOI: 10.3906/kim-1307-66.

[16] Baei, M. T.; Peyghan, A. A.; Bagheri, Z., A DFT study on CO_2 interaction with a BN nano-cage. *Bull. Korean. Chem. Soc.*, **2012**, *33*, 3339. DOI: 10.5012/bkcs.2012.33.10.3338.

[17] Beheshtian, J.; Kamfiroozi, M.; Bagheri, Z.; Peyghan, A. A., $B_{12}N_{12}$ nano-cage as potential sensor for NO_2 detection. *Chinese. J. Chem. Phys.*, **2012**, *25*,

60-64. DOI: 10.1088/1674-0068/25/01/60-64.

[18] Peyghan, A. A.; Soleymanabadi, H., Computational study on ammonia adsorption on the $X_{12}Y_{12}$ nano-clusters (X = B, Al and Y = N, P). *Curr. Sci.*, **2015**, *108*, (00113891).

[19] Soltani, A.; Javan, M. B., Carbon monoxide interactions with pure and doped $B_{11}XN_{12}$ (X = Mg, Ge, Ga) nano-clusters: a theoretical study. *RSC Adv.*, **2015**, *5*, 90621-90631. DOI: 10.1039/C5RA12571E.

[20] Esrafili, M. D.; Nurazar, R., Methylamine adsorption and decomposition on $B_{12}N_{12}$ nanocage: A density functional theory study. *Surf. Sci.*, **2014**, *626*44-48. DOI: 10.1016/j.susc.2014.03.028.

[21] Bahrami, A.; Seidi, S.; Baheri, T.; Aghamohammadi, M., A first-principles study on the adsorption behavior of amphetamine on pristine, P-and Al-doped $B_{12}N_{12}$ nano-cages. *Superlattices. Microstruct.*, **2013**, *64*, 265-273. DOI: 10.1016/ j.spmi.2013.09.034.

[22] Esrafili, M. D.; Nurazar, R., Metal-free decomposition of formic acid on pristine and carbon-doped boron nitride fullerene: A DFT study. *J. Clust. Sci.*, **2015**, *26*, 595-608,

[23] Baei, M. T., $B_{12}N_{12}$ sodalite like cage as potential sensor for hydrogen cyanide. *Comput. Theor. Chem.*, **2013**, *1024*28-33.

[24] Beheshtian, J.; Tabar, M. B.; Bagheri, Z.; Peyghan, A. A., Exohedral and endohedral adsorption of alkaline earth cations in BN nanocluster. J. Mol. Model., **2013**, *19*, 1445-1450. DOI: 10.1007/s00894-012-1702-y.

[25] Wang, H., A density functional investigation of fluorinated $B_{12}N_{12}$ clusters. *Chinese. J. Chem.*, **2010**, *28*, 1897-1901. DOI: 10.1002/cjoc.201090316.

[26] Baei, M. T.; Bagheri, Z.; Peyghan, A. A., Transition metal atom adsorptions on a boron nitride nanocage. *Struct. Chem.*, **2013**, *24*, 1039-1044. DOI: 10.1007/ s11224-012-0132-x.

[27] Li, X. -M.; Tian, W. Q.; Dong, Q.; Huang, X.-R.; Sun, C. -C.; Jiang, L., Substitutional doping of BN nanotube by transition metal: A density functional theory simulation. *Comput. Theor. Chem.*, **2011**, *964*, 199-206. DOI: 10.1016/j.comptc.2010.12.026.

[28] Noei, M.; Arjmand, M., Removal of cyanogen toxic gas from environmental system by using BN nanosheet. *Ind. J. Fund. Appl. Life. Sci.*, **2014**, *5*5074-5080.

[29] Soltani, A.; Baei, M. T.; Lemeski, E. T.; Pahlevani, A. A., The study of SCN^- adsorption on $B_{12}N_{12}$ and $B_{16}N_{16}$ nano-cages. *Superlattices Microstruct.*, **2014**, *5*, 75716-724. DOI: 10.1016/j.spmi.2014.07.038.

[30] Beheshtian, J.; Soleymanabadi, H.; Kamfiroozi, M.; Ahmadi, A., The H_2 dissociation on the BN, AlN, BP and AlP nanotubes: a comparative study. *J. Mol. Model.*, **2012**, *18*, 2343-2348. DOI: 10.1007/s00894-011-1256-4.

[31] Ni, M.; Zeng, Z.; Ju, X., First-principles study of metal atom adsorption on the boron-doped carbon nanotubes. *Microelectr. J.*, **2009**, *40*, 863-866. DOI: 10.1016/j.mejo.2008.11.021.

[32] Beheshtian, J.; Peyghan, A. A.; Bagheri, Z.; Tabar, M. B., Density-functional calculations of HCN adsorption on the pristine and Si-doped graphynes. *Struct. Chem.*, **2014**, *25*, 1-7. DOI: 10.1007/s11224-013-0230-4.

[33] Xu, L. -C.; Li, J.; Shi, S.; Zheng, K. -C.; Ji, L. -N., DFT/TDDFT studies on electronic absorption and emission spectra of $[Ru(bpy)_2 (L)]^{2+}$ (L = pip, o-mopip and p-mopip) in aqueous solution. *J. Mol. Struct.*, **2008**, *855*, 77-81. DOI: 10.1016/ j.theochem.2008.01.003.

[34] Yanai, T.; Tew, D. P.; Handy, N. C., A new hybrid exchange-correlation functional using the Coulomb-attenuating method (CAM-B3LYP). *Chem. Phys. Lett.*, **2004**, *393*, 51-57. DOI: 10.1016/ j.cplett.2004.06.011.

[35] Parr, R. G.; Yang, R. G. P. W., *Density-functional theory of atoms and molecules*. Oxford university press, **1989**.

[36] Reed, A. E.; Weinstock, R. B.; Weinhold, F., Natural population analysis. *J. Chem. Phys.*, **1985**, *83*, 735-746. DOI: 10.1063/1.449486.

[37] Frisch, M.; Trucks, G.; Schlegel, H.; Scuseria, G.; Robb, M.; Cheeseman, J.; Montgomery Jr, J.; Vreven, T.; Kudin, K.; Burant, J., Pittsburgh P. A.; Pople, J. A., (2009) Gaussian 09, revision A02. Gaussian Inc., Wallingford.

[38] Geerlings, P.; De Proft, F.; Langenaeker, W.,

Conceptual density functional theory. *Chem. Rev.*, **2003**, *103*, 1793-1874. DOI: 10.1021/cr990029p.

[39] Parr, R. G.; Donnelly, R. A.; Levy, M.; Palke, W. E., Electronegativity: the density functional viewpoint. *J. Chem. Phys.*, **1978**, *68*, 3801-3807. DOI: 10.1063/1.436185.

[40] Janak, J., Proof that $\partial E/\partial n_i = \varepsilon$ in density-functional theory. *Phys. Rev. B*, **1978**, *18*, 7165. DOI: 10.1103/PhysRevB.18.7165.

[41] Parr, R. G.; Szentpaly, L. V.; Liu, S., Electrophilicity index. *J. Am. Chem. Soc.*, **1999**, *121*, 1922-1924. DOI: 10.1021/ja983494x.

[42] O'boyle, N. M.; Tenderholt, A. L.; Langner, K. M., Cclib: a library for package-independent computational chemistry algorithms. *J. Comput. Chem.*, **2008**, *29*, 839-845. DOI: 10.1002/jcc.20823.

[43] Turi, L.; Dannenberg, J., Correcting for basis set superposition error in aggregates containing more than two molecules: ambiguities in the calculation of the counterpoise correction. *J. Phys. Chem.*, **1993**, *97*, 2488-2490. DOI: 10.1021/j100113a002.

[44] Wang, Q.; Sun, Q.; Jena, P.; Kawazoe, Y., Potential of AlN nanostructures as hydrogen storage materials. *ACS nano*, **2009**, *3*, 621-626. DOI: 10.1021/nn800815e.

[45] Furche, F.; Ahlrichs, R., Adiabatic time-dependent density functional methods for excited state properties. *J. Chem. Phys.*, **2002**, *117*, 7433-7447. DOI: 10.1063/1.1508368.

[46] Lan, Y. -Z.; Cheng, W. -D.; Wu, D. -S.; Li, X. -D.; Zhang, H.; Gong, Y. -J.; Shen, J.; Li, F.-F., Theoretical studies of third-order nonlinear optical response for $B_{12}N_{12}$, $B_{24}N_{24}$ and $B_{36}N_{36}$ clusters. *J. Mol. Struct.*, **2005**, *730*, 9-15. DOI: 10.1016/j.theochem.2005.06.008.

[47] Møller, C.; Stoicheff, B., High resolution raman spectroscopy of gases: IV. rotational raman spectrum of cyanogen. *Can. J. Phys.*, **1954**, *32*, 635-638. DOI: 10.1139/p54-067.

[48] Leenaerts, O.; Partoens, B.; Peeters, F., Adsorption of H_2O, NH_3, CO, NO_2, and NO on graphene: A first-principles study. *Phys. Rev. B*, **2008**, *77*, 125416. DOI: 10.1103/PhysRevB.77.125416.

[49] Dai, J.; Yuan, J.; Giannozzi, P., Gas adsorption on graphene doped with B, N, Al and S: a theoretical study. *Appl. Phys. Lett.*, **2009**, *95*, 232105. DOI: 10.1063/1.3272008.

[50] Carrillo, I.; Rangel, E.; Magaña, L., Adsorption of carbon dioxide and methane on graphene with a high titanium coverage. *Carbon.*, **2009**, *47*, 2758-2760. DOI: 10.1016/j.carbon.2009.06.022.

[51] Beheshtian, J.; Peyghan, A. A.; Bagheri, Z., Detection of phosgene by Sc-doped BN nanotubes: a DFT study. *Sens. Actuators. B*, **2012**, *171*, 846-852. DOI: 10.1016/j.snb.2012.05.082.

[52] Alwarappan, S.; Kumar, A., *Graphene-based Materials: Science and Technology*. CRC Press, **2013**. p.